Letter

Quantum phases in the honeycomb-lattice J_1–J_3 ferro-antiferromagnetic model

Shengtao Jiang (蒋晟韬), Steven R. White, and A. L. Chernyshev
Department of Physics and Astronomy, University of California, Irvine, California 92697, USA

(Received 7 April 2023; accepted 2 November 2023; published 14 November 2023)

Using large-scale density-matrix renormalzation group calculations and minimally augmented spin-wave theory, we demonstrate that the phase diagram of the quantum $S=\frac{1}{2}$ J_1–J_3 ferro-antiferromagnetic model on the honeycomb lattice differs dramatically from the classical one. It hosts the double-zigzag and Ising-z phases as unexpected intermediaries between ferromagnetic and zigzag states that are also extended beyond their classical regions of stability. In broad agreement with quantum order-by-disorder arguments, these collinear phases replace the classical spiral state.

DOI: 10.1103/PhysRevB.108.L180406

Introduction. Ever since the Anderson's seminal work on the resonating valence-bond state [1], the significant role that can be played by quantum fluctuations in magnets with competing interactions has remained at the forefront of condensed matter physics, inspiring a multitude of quests for exotic states, models that can realize them, and real materials that can host them [2–7]. The elusive spin-liquid states with strongly entangled spins are but one example [2]; others include valence-bond phases with spatial symmetry breaking [8–14], quantum multipolar spin nematics that are quantum analogues of liquid crystals [15–18], and an especially extensive class of unconventional magnetically *ordered* phases that do not appear in the classical solutions of the underlying spin models [19–28]. It is the latter group of phenomena that creates a broader context for the present study.

The ordered phases that are not favored classically but are stabilized in the quantum $S=\frac{1}{2}$ limit have attracted significant attention in the search for Kitaev magnets on the honeycomb lattice [29–32]. Recently, this extensive experimental and theoretical effort has expanded to the Co^{2+} materials [33–46]. It appears that the minimal XXZ-anisotropic J_1–J_3 model with "mixed" ferro-antiferromagnetic (FM-AFM) couplings, given by

$$H=\sum_{n=1,3}\sum_{\langle ij\rangle_n} J_n\left(S_i^xS_j^x+S_i^yS_j^y+\Delta_nS_i^zS_j^z\right), \qquad (1)$$

provides a tantalizingly close description for many of these compounds [43–49], calling for its unbiased study. Here $\langle ij\rangle_{1(3)}$ stands for the first-(third-)neighbor bonds, $J_1=-1$ is the energy unit, $J_3>0$, and $0\leqslant\Delta_n\leqslant 1$ are the XXZ anisotropies. We note that earlier pre-Kitaev searches for exotic quantum states have focused on a pure AFM J_1–J_2–J_3 honeycomb-lattice model [50–61], motivated by the expectation of stronger fluctuations due to the lattice's low coordination number and by the degeneracies in its classical phase diagram [53].

The model (1) was studied in the 1970s [62], yielding the classical phase diagram reproduced in Fig. 1(a). These phases are independent of Δ_n because all relevant classical states are coplanar. The ground state is FM for small J_3, while zigzag (ZZ) order is preferred for large J_3, and the ferrimagnetic spiral phase (Sp) continuously interpolates between FM and ZZ.

In this Letter, we combine density-matrix renormalization group (DMRG) and minimally-augmented spin-wave theory (MAGSWT) to obtain the ground-state phase diagram of the quantum $S=\frac{1}{2}$ model (1). We focus on the *partial* XXZ version of the model (1), with the J_3 term left in the Heisenberg limit, $\Delta_3=1$, referred to as the J_1^{Δ}–J_3 model. This choice is motivated by real materials, in which further exchanges tend to be more isotropic [32,63]. The standard version of the model with equal anisotropies, $\Delta_1=\Delta_3$, referred to as the *full* XXZ or J_1^{Δ}–J_3^{Δ} model, is considered too.

Phase diagram. Our phase diagram for the $S=\frac{1}{2}$ J_1^{Δ}–J_3 model is given in Fig. 1(b). In a dramatic deviation from the classical case, we find two unconventional phases stabilized by quantum fluctuations—the double-zigzag (dZZ) and Ising-z (Iz) phases—as intermediary between the FM and ZZ phases. The FM and ZZ phases also extend well beyond their classical regions to completely supersede the noncollinear classical spiral phase.

The solid lines are phase boundaries interpolating transition points obtained from the DMRG long-cylinder DMRG "scans" by varying J_3 or Δ, as well as from the more precise measurements. The dashed lines are phase boundaries of the same phases obtained by MAGSWT, with both approaches described below.

The qualitative agreement between these approaches is quite remarkable. Both methods produce the classically unstable dZZ and Iz phases, both expand the FM and ZZ phases beyond their classical ranges, and both eliminate the Sp phase. These findings are also in a broad agreement with order-by-disorder arguments [20,27], which generally favor collinear phases.

We note that recent studies of related models also found the Sp phase to be absent [64,65]. However, our conclusions on the nature and extent of the quantum phases that replace it differ substantially from theirs. For the details on these differences for the J_1–J_3 and other models, see the Supplemental Material (SM) [66] and the discussions below.

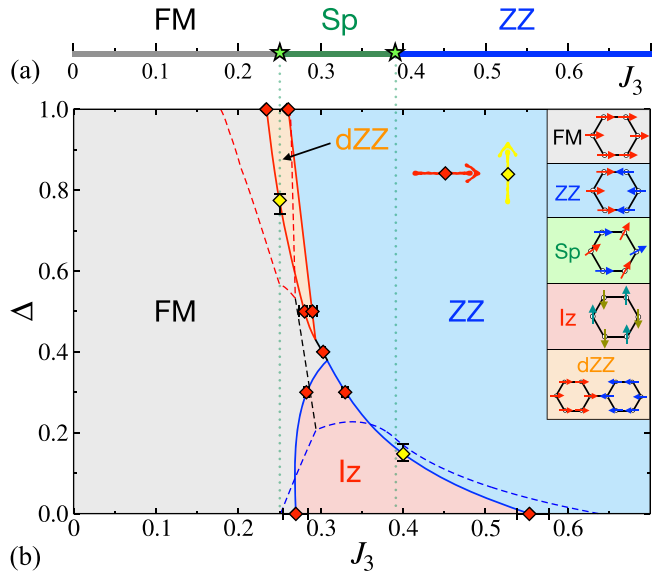

FIG. 1. The classical (a) and quantum (b) phase diagrams of the XXZ J_1^{Δ}–J_3 model (1) with the ferromagnetic (FM), zigzag (ZZ), spiral (Sp), double-zigzag (dZZ), and Ising-z (Iz) phases. The solid lines are phase boundaries interpolating transition points (diamonds) inferred from the DMRG scans along J_3 (red) and Δ (yellow). The vertical and dashed lines are classical and MAGSWT phase boundaries, respectively. Spins are in-plane for all phases except Iz, see also Fig. 2.

The $U(1)$-preserving Iz phase, with spins ordered Néel-like along the z axis, has been first discovered in the XY J_1-J_2 AFM-AFM model [60], where Iz order is stabilized solely by quantum effects with no exchange coupling favoring it. In our case, we find the z axis component of the J_3 exchange in the J_1^{Δ}-J_3 model crucial for stabilizing the Iz phase in a wide range of parameters, see Fig. 1(b). In contrast to Ref. [65], we find only a very narrow Iz phase in the J_1^{Δ}-J_3^{Δ} model. The spin-liquid phases in this model [64,65] are also not supported (see the SM [66]).

The dZZ phase has been recently reported experimentally [43] and found favored by the *bond-dependent* extensions of the XY J_1^{Δ}–J_3^{Δ} model [45,46]. Instead, we find the dZZ phase already in the Heisenberg limit of the principal J_1–J_3 model (1), see Fig. 1(b).

DMRG calculations. DMRG calculations were performed on the $L_x \times L_y$-site honeycomb-lattice open cylinders of width L_y up to 16 (8 honeycomb cells), using the ITensor library [67]. The majority of the results were obtained on the so-called X cylinders (XC) [59], in which the first-neighbor bond is horizontal, while both X and Y cylinders (YC) were used for more delicate phases [68]. We allow for a spontaneous breaking of the spin $U(1)$ symmetry [69], enabling us to measure the local ordered moment $\langle \mathbf{S}_i \rangle$ instead of the correlation function.

Our main exploratory tool is the long-cylinder "scans," in which one parameter, J_3 or Δ, is varied along the length of the cylinder with L_x up to 40. It provides 1D cuts through the 2D phase diagram [60,70–72], see Fig. 2, which give approximate phase boundaries. By narrowing parameter ranges of the scans one can determine the boundaries with increased precision, distinguish first- and second-order transitions [15], and uncover hidden phases. In cases when the phase boundary is less obvious, we utilize the fixed parameter (nonscan) calculations on clusters up to 16×16, with the aspect ratio that closely approximates the 2D thermodynamic limit [73].

In Fig. 2, we present two long-cylinder scans for the J_1^{Δ}–J_3 model (1), one in the Heisenberg limit, $\Delta = 1$, and the other in the XY limit, $\Delta = 0$, vs J_3. In the Heisenberg limit, Fig. 2(a), the transition from FM to ZZ is very sharp and FM phase seems to terminate right at the classical boundary of this state, $J_3^{cl} = 0.25$. However, one would expect that the FM phase should retreat from this boundary, as the competing ZZ state

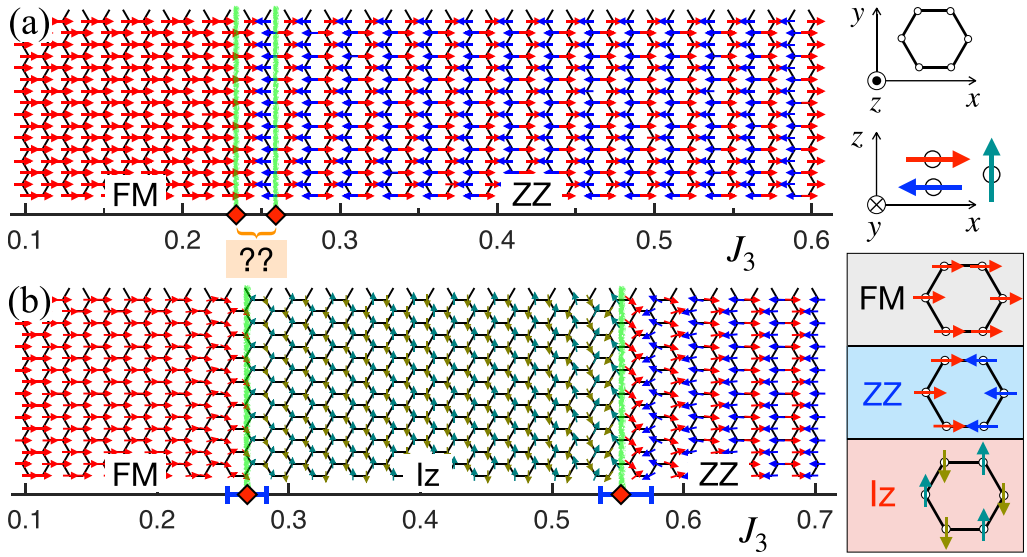

FIG. 2. Long-cylinder scans of the J_1^{Δ}–J_3 model (1) vs J_3 in the (a) Heisenberg ($\Delta = 1$) and (b) XY ($\Delta = 0$) limit. The arrows show the local ordered moment $\langle \mathbf{S}_i \rangle$. FM, ZZ, and Iz phases are indicated and transitions are determined as described in text. The honeycomb lattice is in the xy plane while spins shown in the figure are in the xz plane.

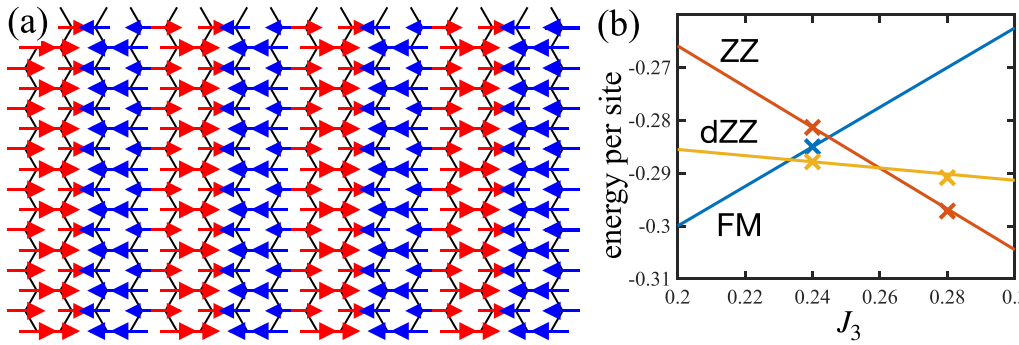

FIG. 3. (a) Ordered moments in the 16×16 nonscan cluster for $J_3=0.24$, showing dZZ pattern. (b) Energies of the three competing phases vs J_3, crosses are DMRG results and higher-energy states are metastable. Lines are extrapolated energies, $\langle\psi_i|H(J_3)|\psi_i\rangle$, where ψ_i are the three states at $J_3=0.24$.

is fluctuating in the Heisenberg limit, while the FM state is exact. The subsequent analysis reveals a hidden intermediate dZZ state, discussed next. We note that the scan calculation in Fig. 2(a) misses it not only due to the narrow region of the dZZ phase, but also because of the high symmetry of the model in the Heisenberg limit, which requires additional effort to avoid metastable states.

Figure 2(b) for the XY limit shows transitions from the FM to Iz and from Iz to ZZ vs J_3. By using scans in the narrower ranges of J_3, we verify that the spiral-like spin patterns in the transition regions in Fig. 2(b) are proximity effects of the neighboring phases, not additional phases. The phase boundaries shown in Fig. 2(b) and used in the phase diagram in Fig. 1(b) are the crossing points of the order parameters vs J_3 (see the SM [66]). The error bars are the width of the transition region in the scans, where a discontinuous transition is assigned a width equal to the parameter change over one lattice spacing.

In the Heisenberg limit, the three states, FM, dZZ, and ZZ, compete in the proximity of the classical FM boundary $J_3=0.25$. Because of the high spin symmetry of the model, and depending on the initial state, all three can be stabilized in the nonscan DMRG simulations, such as the one shown in Fig. 3(a) for $J_3=0.24$ in the 16×16 cluster. As is shown in Fig. 3(b), the energy of the dZZ is the lowest, with the FM and ZZ being metastable, suggesting that the transitions between the corresponding phases are first order. To identify their phase boundaries, we compare the energies of these three states as a function of J_3 using extrapolations based on the spin-spin correlations extracted at $J_3=0.24$ from the center of the cluster for each of the states. While the FM line is exact in this limit, the extrapolated energies for ZZ and dZZ are also very close to the ones given by a direct DMRG calculation at a different value of J_3, justifying the analysis, see Fig. 3(b). The dZZ phase is found to be confined between $J_3=0.2333$ and 0.2596.

The lower spin symmetry away from the Heisenberg limit helps to reveal the dZZ phase more readily, see Fig. 4(a) for a long-cylinder scan along the Δ axis and fixed $J_3=0.25$, confirming the presence of this phase in an extended region of the phase diagram in Fig. 1. A similar Δ scan for $J_3=0.4$ in Fig. 4(b) compliments the J_3 scans in establishing boundaries of the Iz phase.

By using a combination of the narrower ranges of the scans and fixed-parameter nonscans, we find that the dZZ phase persists somewhat below $\Delta=0.5$ while the Iz phase ends close to $\Delta=0.4$, where the FM-to-ZZ transition appears to be direct, see Fig. 1 and the SM [66]. Although we cannot completely rule out the Iz state for $\Delta=0.4$, it must be extremely narrow if it exists.

Minimally-augmented spin-wave theory. The standard SWT is successful at accounting for quantum effects in the ordered states [74], but cannot describe either the ordered phases that are not classically stable, or the shifts of the phase boundaries by quantum fluctuations. An analytical approach to address this problem, originally proposed for the classically unstable field-induced states in the transverse-field Ising and frustrated Heisenberg models [75–77], can be successfully applied here.

The method consists of introducing a local field in the direction of the ordered moment $\mathbf{n}_i$ for the proposed (unstable) classical spin configurations, leading to a shift of the chemical potential in the bosonic SWT language

$$\delta\mathcal{H}=\mu\sum_i(S-\mathbf{S}_i\cdot\mathbf{n}_i)=\mu\sum_i a_i^\dagger a_i, \tag{2}$$

while leaving the classical energy of the state unchanged. The *minimal* value of μ is chosen to ensure stability of the spectrum, i.e., that the squares of all eigenvalues of the SWT matrix are positive definite. Then, the energy of the proposed spin state, $\mathcal{E}=E_{cl}+\delta E$, with the $1/S$ correction to the ground-state energy δE, is well defined and can be compared with the energies of the competing states calculated to the same $O(S)$ order.

The power of the method, coined as the *minimally augmented SWT* (MAGSWT), is not only in its simplicity, but in the form of Eq. (2), which guarantees that its contribution to the Hamiltonian is positive for $\mu>0$. In turn, this implies that the so-obtained ground-state energy $\mathcal{E}$ is an *upper bound* for the energy of the suggested spin state to the order $O(S)$. This method allows one to consider the phase beyond its classical range of stability and inspect states that are classically not competitive, but can lower their energy due to quantum fluctuations. The new phase boundaries are determined from the crossings of the energies $\mathcal{E}$ for the competing phases as a function of the varied parameter(s).

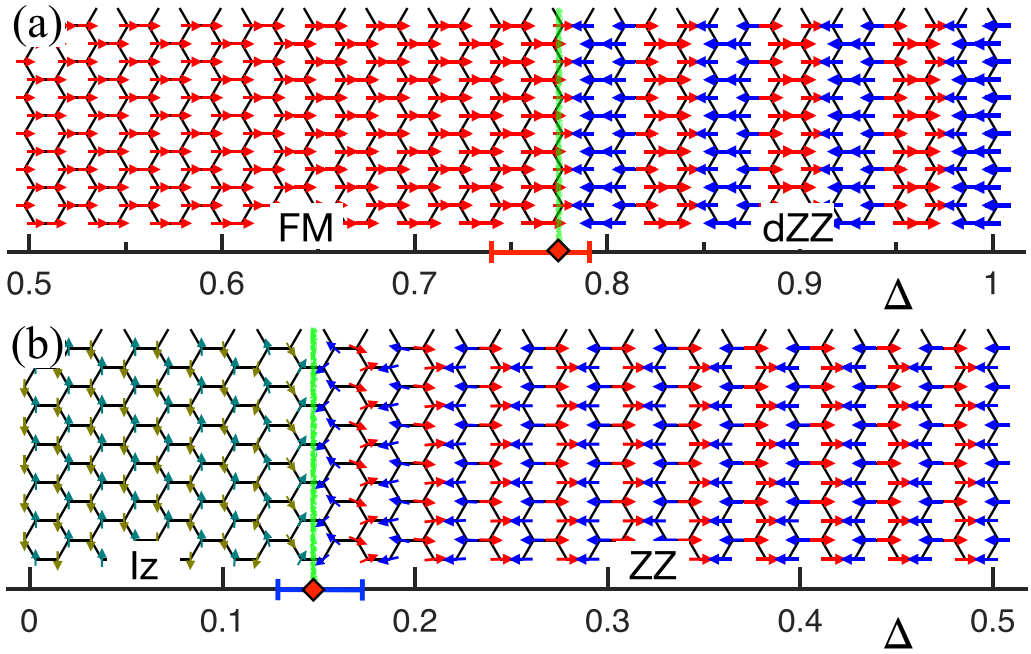

FIG. 4. Long-cylinder Δ scans of the J_1^{Δ}–J_3 model (1) for (a) $J_3=0.25$ and (b) $J_3=0.4$. Notations are as in Fig. 2.

We note that MAGSWT may not be applied to an arbitrary classically unstable state [77], with the absence of the linear-bosonic terms in the $1/S$ expansion for a given state being a sufficient criterion of its applicability.

MAGSWT results. In case of the XXZ J_1^{Δ}–J_3 model (1), all four competing phases of interest are collinear, which guarantees the absence of the linear-bosonic terms, while the noncollinear Sp state is not the subject of MAGSWT, as it corresponds to a minimum of the classical energy in its entire possible range of existence.

The technical procedure of extracting minimal μ vs J_3 and Δ for each phase is discussed in the SM [66]. We note that the limiting XY and Heisenberg cases and select momenta are useful for obtaining analytical expressions for $\mu(J_3, \Delta)$, eliminating the need of a numerical scan of the momentum space for spectrum instabilities. With that, the energy surfaces $\mathcal{E}(J_3, \Delta)$ are readily obtained for each phase and the MAGSWT phase boundaries are drawn from the intersections of such surfaces.

The resulting phase boundaries are shown in Fig. 1(b) by the dashed lines. Most, if not all, of the features already discussed above are present. The noncollinear Sp phase is not effective at benefiting from quantum fluctuations, in agreement with the order-by-disorder arguments [20], and is wiped out. The classically unstable dZZ and Iz phases are extensive and both FM and ZZ expand beyond their classical borders. A close quantitative agreement with the DMRG phase boundaries can also be observed, with most discrepancies concerning the borders of the less-fluctuating FM phase (see the SM [66]). Otherwise, the entire picture for the J_1^{Δ}–J_3 model in Fig. 1(b) is in rather astonishing agreement with the numerical data.

The J_1^{Δ}–J_3^{Δ} model. The phase diagram of the full XXZ model (1) with equal anisotropies in both terms, obtained using the same methods as described above, is presented in Fig. 5. It repeats most of the trends of the partial XXZ model in Fig. 1(b), such as the absence of the Sp phase, expansion of the FM and ZZ, and the presence of the two unconventional phases, Iz and dZZ.

In contrast to the recent studies [64,65], our results do not support the proposed spin-liquid states in the Heisenberg [65], or strongly anisotropic ($\Delta=0.25$) nearly XY [64] limits. The J_3 width of the quantum Iz phase in the same XY limit ($\Delta=0$) is also an order of magnitude narrower in our case than the one suggested in Ref. [65].

While the first of the quantum phases, dZZ, missed by the previous studies due to small cluster sizes or an approximate nature of their approaches [65], is nearly the same in the partial and full XXZ models in Fig. 1(b) and Fig. 5, respectively,

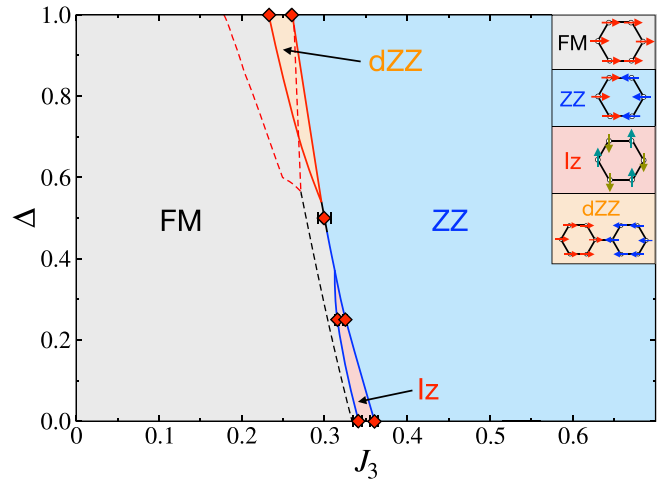

FIG. 5. The quantum $S=\frac{1}{2}$ phase diagrams of the full XXZ J_1^{Δ}–J_3^{Δ} model (1), c.f. Fig. 1(b). See text.

the Iz phase is substantially more tenuous. In fact, the initial DMRG scans have shown a direct FM-ZZ transition, with some possible narrow intermediate state. Dedicated nonscans in that region did uncover short-range correlations in both XC and YC clusters [66], not unlike the ones reported in Ref. [64]. However, these spin-liquid suspects either order on the cylinder width increase (XC), or indicate a sufficiently robust Iz order in the range of $J_3 = 0.315$–0.325 for $\Delta = 0.25$ and $J_3 = 0.34$–0.36 for $\Delta = 0$, see [66].

It is worth noting that MAGSWT in the XY limit of the full XXZ model shows a close, but insufficient, competition of the strongly fluctuating Iz phase, rendering it absent from its version of the phase diagram in Fig. 5.

Summary. In this Letter, we have studied the emergence of the quantum phases that are not stable classically within a simple model of great current interest. We have combined state-of-the-art DMRG and analytical approaches to obtain conclusive phase diagrams of this model. It is established beyond any reasonable doubt that the two unconventional quantum phases occupy a significant portion of this diagram, with the known phases also extending well beyond their classical regions and completely replacing the less-fluctuating noncollinear phase. The results of the analytical MAGSWT approach are shown to be in a close accord with the numerical DMRG data, providing additional insights into the energetics of the quantum stabilization of the nonclassical phases and offering a systematic path for the explorations of similar models.

The proposed phase diagrams have direct relevance to a group of novel materials and provide important guidance to the ongoing theoretical and experimental searches of the unconventional quantum states.

Acknowledgments. We are sincerely thankful to Arun Paramekanti for several important discussions and numerous exchanges. We are grateful to Ciarán Hickey, Simon Trebst, and Yoshito Watanabe for the kind remarks and useful conversations. The work of S.J. and S.R.W. was supported by the NSF through Grant No. DMR-2110041. The inception of the paper, key analysis, and analytical and numerical calculations using MAGSWT by A.L.C. were supported by the U.S. Department of Energy, Office of Science, Basic Energy Sciences under Award No. DE-SC0021221.

[1] P. Anderson, Resonating valence bonds: A new kind of insulator? Mater. Res. Bull. **8**, 153 (1973).
[2] L. Balents, Spin liquids in frustrated magnets, Nature (London) **464**, 199 (2010).
[3] M. R. Norman, Colloquium: Herbertsmithite and the search for the quantum spin liquid, Rev. Mod. Phys. **88**, 041002 (2016).
[4] Y. Zhou, K. Kanoda, and T.-K. Ng, Quantum spin liquid states, Rev. Mod. Phys. **89**, 025003 (2017).
[5] J. Knolle and R. Moessner, A field guide to spin liquids, Annu. Rev. Condens. Matter Phys. **10**, 451 (2019).
[6] A. Kitaev, Anyons in an exactly solved model and beyond, Ann. Phys. **321**, 2 (2006).
[7] L. Capriotti, F. Becca, A. Parola, and S. Sorella, Resonating valence bond wave functions for strongly frustrated spin systems, Phys. Rev. Lett. **87**, 097201 (2001).
[8] V. Zapf, M. Jaime, and C. D. Batista, Bose-Einstein condensation in quantum magnets, Rev. Mod. Phys. **86**, 563 (2014).
[9] M. Mambrini, A. Läuchli, D. Poilblanc, and F. Mila, Plaquette valence-bond crystal in the frustrated Heisenberg quantum antiferromagnet on the square lattice, Phys. Rev. B **74**, 144422 (2006).
[10] S.-S. Gong, W. Zhu, D. N. Sheng, O. I. Motrunich, and M. P. A. Fisher, Plaquette ordered phase and quantum phase diagram in the spin-$\frac{1}{2}$ J_1–J_2 square Heisenberg model, Phys. Rev. Lett. **113**, 027201 (2014).
[11] K. Kodama, M. Takigawa, M. Horvatić, C. Berthier, H. Kageyama, Y. Ueda, S. Miyahara, F. Becca, and F. Mila, Magnetic superstructure in the two-dimensional quantum antiferromagnet $SrCu_2(BO_3)_2$, Science **298**, 395 (2002).
[12] Y. H. Matsuda, N. Abe, S. Takeyama, H. Kageyama, P. Corboz, A. Honecker, S. R. Manmana, G. R. Foltin, K. P. Schmidt, and F. Mila, Magnetization of $SrCu_2(BO_3)_2$ in ultrahigh magnetic fields up to 118 T, Phys. Rev. Lett. **111**, 137204 (2013).
[13] M. Jaime, R. Daou, S. A. Crooker, F. Weickert, A. Uchida, A. E. Feiguin, C. D. Batista, H. A. Dabkowska, and B. D. Gaulin, Magnetostriction and magnetic texture to 100.75 Tesla in frustrated $SrCu_2(BO_3)_2$, Proc. Natl. Acad. Sci. USA **109**, 12404 (2012).
[14] F. Ferrari, S. Bieri, and F. Becca, Competition between spin liquids and valence-bond order in the frustrated spin-$\frac{1}{2}$ Heisenberg model on the honeycomb lattice, Phys. Rev. B **96**, 104401 (2017).
[15] S. Jiang, J. Romhányi, S. R. White, M. E. Zhitomirsky, and A. L. Chernyshev, Where is the quantum spin nematic? Phys. Rev. Lett. **130**, 116701 (2023).
[16] M. E. Zhitomirsky and H. Tsunetsugu, Magnon pairing in quantum spin nematic, Europhys. Lett. **92**, 37001 (2010).
[17] K. Penc and A. M. Läuchli, Spin nematic phases in quantum spin systems, in *Introduction to Frustrated Magnetism: Materials, Experiments, Theory*, edited by C. Lacroix, P. Mendels, and F. Mila (Springer-Verlag, Berlin Heidelberg, 2011), p. 331.
[18] Y. Kohama, H. Ishikawa, A. Matsuo, K. Kindo, N. Shannon, and Z. Hiroi, Possible observation of quantum spin-nematic phase in a frustrated magnet, Proc. Natl. Acad. Sci. USA **116**, 10686 (2019).
[19] C. L. Henley, Ordering by disorder: Ground-state selection in fcc vector antiferromagnets, J. Appl. Phys. **61**, 3962 (1987).
[20] C. L. Henley, Ordering due to disorder in a frustrated vector antiferromagnet, Phys. Rev. Lett. **62**, 2056 (1989).
[21] O. A. Starykh, Unusual ordered phases of highly frustrated magnets: A review, Rep. Prog. Phys. **78**, 052502 (2015).
[22] A. W. C. Wong, Z. Hao, and M. J. P. Gingras, Ground state phase diagram of generic XY pyrochlore magnets with quantum fluctuations, Phys. Rev. B **88**, 144402 (2013).
[23] K. A. Ross, L. Savary, B. D. Gaulin, and L. Balents, Quantum excitations in quantum spin ice, Phys. Rev. X **1**, 021002 (2011).
[24] J. G. Rau and M. J. Gingras, Frustrated quantum rare-earth pyrochlores, Annu. Rev. Condens. Matter Phys. **10**, 357 (2019).

[25] A. M. Hallas, J. Gaudet, and B. D. Gaulin, Experimental insights into ground-state selection of quantum XY pyrochlores, Annu. Rev. Condens. Matter Phys. **9**, 105 (2018).

[26] J. G. Rau, R. Moessner, and P. A. McClarty, Magnon interactions in the frustrated pyrochlore ferromagnet $Yb_2Ti_2O_7$, Phys. Rev. B **100**, 104423 (2019).

[27] J. G. Rau, P. A. McClarty, and R. Moessner, Pseudo-Goldstone gaps and order-by-quantum disorder in frustrated magnets, Phys. Rev. Lett. **121**, 237201 (2018).

[28] R. Schick, O. Götze, T. Ziman, R. Zinke, J. Richter, and M. E. Zhitomirsky, Ground-state selection by magnon interactions in a FCC antiferromagnet, Phys. Rev. B **106**, 094431 (2022).

[29] W. Witczak-Krempa, G. Chen, Y. B. Kim, and L. Balents, Correlated quantum phenomena in the strong spin-orbit regime, Annu. Rev. Condens. Matter Phys. **5**, 57 (2014).

[30] R. Schaffer, E. K.-H. Lee, B.-J. Yang, and Y. B. Kim, Recent progress on correlated electron systems with strong spin-orbit coupling, Rep. Prog. Phys. **79**, 094504 (2016).

[31] J. G. Rau, E. K.-H. Lee, and H.-Y. Kee, Spin-orbit physics giving rise to novel phases in correlated systems: Iridates and related materials, Annu. Rev. Condens. Matter Phys. **7**, 195 (2016).

[32] S. M. Winter, A. A. Tsirlin, M. Daghofer, J. van den Brink, Y. Singh, P. Gegenwart, and R. Valentí, Models and materials for generalized Kitaev magnetism, J. Phys.: Condens. Matter **29**, 493002 (2017).

[33] H. Liu and G. Khaliullin, Pseudospin exchange interactions in d^7 cobalt compounds: Possible realization of the Kitaev model, Phys. Rev. B **97**, 014407 (2018).

[34] H. Liu, J. Chaloupka, and G. Khaliullin, Kitaev spin liquid in 3d transition metal compounds, Phys. Rev. Lett. **125**, 047201 (2020).

[35] X. Zhang, Y. Xu, T. Halloran, R. Zhong, C. Broholm, R. Cava, N. Drichko, and N. Armitage, A magnetic continuum in the cobalt-based honeycomb magnet $BaCo_2(AsO_4)_2$, Nat. Mater. **22**, 58 (2023).

[36] R. Zhong, T. Gao, N. P. Ong, and R. J. Cava, Weak-field induced nonmagnetic state in a Co-based honeycomb, Sci. Adv. **6**, eaay6953 (2020).

[37] H. S. Nair, J. M. Brown, E. Coldren, G. Hester, M. P. Gelfand, A. Podlesnyak, Q. Huang, and K. A. Ross, Short-range order in the quantum XXZ honeycomb lattice material $BaCo_2(PO_4)_2$, Phys. Rev. B **97**, 134409 (2018).

[38] X. Wang, R. Sharma, P. Becker, L. Bohatý, and T. Lorenz, Single-crystal study of the honeycomb XXZ magnet $BaCo_2(PO_4)_2$ in magnetic fields, Phys. Rev. Mater. **7**, 024402 (2023).

[39] H. Yang, C. Kim, Y. Choi, J. H. Lee, G. Lin, J. Ma, M. Kratochvílová, P. Proschek, E.-G. Moon, K. H. Lee, Y. S. Oh, and J.-G. Park, Significant thermal Hall effect in the 3d cobalt Kitaev system $Na_2Co_2TeO_6$, Phys. Rev. B **106**, L081116 (2022).

[40] W. Yao, Y. Zhao, Y. Qiu, C. Balz, J. R. Stewart, J. W. Lynn, and Y. Li, Magnetic ground state of the Kitaev $Na_2Co_2TeO_6$ spin liquid candidate, Phys. Rev. Res. **5**, L022045 (2023).

[41] M. Songvilay, J. Robert, S. Petit, J. A. Rodriguez-Rivera, W. D. Ratcliff, F. Damay, V. Balédent, M. Jiménez-Ruiz, P. Lejay, E. Pachoud, A. Hadj-Azzem, V. Simonet, and C. Stock, Kitaev interactions in the Co honeycomb antiferromagnets $Na_3Co_2SbO_6$ and $Na_2Co_2TeO_6$, Phys. Rev. B **102**, 224429 (2020).

[42] X. Li, Y. Gu, Y. Chen, V. O. Garlea, K. Iida, K. Kamazawa, Y. Li, G. Deng, Q. Xiao, X. Zheng, Z. Ye, Y. Peng, I. A. Zaliznyak, J. M. Tranquada, and Y. Li, Giant magnetic in-plane anisotropy and competing instabilities in $Na_3Co_2SbO_6$, Phys. Rev. X **12**, 041024 (2022).

[43] L.-P. Regnault, C. Boullier, and J. Lorenzo, Polarized-neutron investigation of magnetic ordering and spin dynamics in $BaCo_2(AsO_4)_2$ frustrated honeycomb-lattice magnet, Heliyon **4**, e00507 (2018).

[44] S. Das, S. Voleti, T. Saha-Dasgupta, and A. Paramekanti, XY magnetism, Kitaev exchange, and long-range frustration in the $J_{\rm eff} = \frac{1}{2}$ honeycomb cobaltates, Phys. Rev. B **104**, 134425 (2021).

[45] P. A. Maksimov, A. V. Ushakov, Z. V. Pchelkina, Y. Li, S. M. Winter, and S. V. Streltsov, *Ab initio* guided minimal model for the "Kitaev" material $BaCo_2(AsO_4)_2$: Importance of direct hopping, third-neighbor exchange, and quantum fluctuations, Phys. Rev. B **106**, 165131 (2022).

[46] T. Halloran, F. Desrochers, E. Z. Zhang, T. Chen, L. E. Chern, Z. Xu, B. Winn, M. Graves-Brook, M. B. Stone, A. I. Kolesnikov, Y. Qiu, R. Zhong, R. Cava, Y. B. Kim, and C. Broholm, Geometrical frustration versus Kitaev interactions in $BaCo_2(AsO_4)_2$, Proc. Natl. Acad. Sci. USA **120**, e2215509119 (2023).

[47] P. A. Maksimov and A. L. Chernyshev, Rethinking α-$RuCl_3$, Phys. Rev. Res. **2**, 033011 (2020).

[48] L. Regnault and J. Rossat-Mignod, Phase transitions in quasi two-dimensional planar magnets, in *Magnetic Properties of Layered Transition Metal Compounds* (Springer, New York, 1990), pp. 271–321.

[49] A. L. Chernyshev, M. E. Zhitomirsky, N. Martin, and L.-P. Regnault, Lifetime of gapped excitations in a collinear quantum antiferromagnet, Phys. Rev. Lett. **109**, 097201 (2012).

[50] Z. Weihong, J. Oitmaa, and C. J. Hamer, Second-order spin-wave results for the quantum XXZ and XY models with anisotropy, Phys. Rev. B **44**, 11869 (1991).

[51] R. R. P. Singh, Z. Weihong, C. J. Hamer, and J. Oitmaa, Dimer order with striped correlations in the J_1–J_2 Heisenberg model, Phys. Rev. B **60**, 7278 (1999).

[52] J. Fouet, P. Sindzingre, and C. Lhuillier, An investigation of the quantum J_1-J_2-J_3 model on the honeycomb lattice, Eur. Phys. J. B **20**, 241 (2001).

[53] A. Mulder, R. Ganesh, L. Capriotti, and A. Paramekanti, Spiral order by disorder and lattice nematic order in a frustrated Heisenberg antiferromagnet on the honeycomb lattice, Phys. Rev. B **81**, 214419 (2010).

[54] J. Oitmaa and R. R. P. Singh, Phase diagram of the $J_1 - J_2 - J_3$ Heisenberg model on the honeycomb lattice: A series expansion study, Phys. Rev. B **84**, 094424 (2011).

[55] D. C. Cabra, C. A. Lamas, and H. D. Rosales, Quantum disordered phase on the frustrated honeycomb lattice, Phys. Rev. B **83**, 094506 (2011).

[56] C. N. Varney, K. Sun, V. Galitski, and M. Rigol, Kaleidoscope of exotic quantum phases in a frustrated XY model, Phys. Rev. Lett. **107**, 077201 (2011).

[57] P. H. Y. Li, R. F. Bishop, and C. E. Campbell, Phase diagram of a frustrated spin-$\frac{1}{2}$ J_1-J_2 XXZ model on the honeycomb lattice, Phys. Rev. B **89**, 220408(R) (2014).

[58] S.-S. Gong, D. N. Sheng, O. I. Motrunich, and M. P. A. Fisher, Phase diagram of the spin-$\frac{1}{2}$ J_1-J_2 Heisenberg model on a honeycomb lattice, Phys. Rev. B **88**, 165138 (2013).

[59] Z. Zhu, D. A. Huse, and S. R. White, Weak plaquette valence bond order in the S=1/2 honeycomb J_1−J_2 Heisenberg model, Phys. Rev. Lett. **110**, 127205 (2013).

[60] Z. Zhu, D. A. Huse, and S. R. White, Unexpected z-direction Ising antiferromagnetic order in a frustrated spin-1/2 $J_1 - J_2$ XY model on the honeycomb lattice, Phys. Rev. Lett. **111**, 257201 (2013).

[61] R. Ganesh, J. van den Brink, and S. Nishimoto, Deconfined criticality in the frustrated Heisenberg honeycomb antiferromagnet, Phys. Rev. Lett. **110**, 127203 (2013).

[62] E. Rastelli, A. Tassi, and L. Reatto, Non-simple magnetic order for simple Hamiltonians, Physica B + C **97**, 1 (1979).

[63] S. M. Winter, Y. Li, H. O. Jeschke, and R. Valentí, Challenges in design of Kitaev materials: Magnetic interactions from competing energy scales, Phys. Rev. B **93**, 214431 (2016).

[64] A. Bose, M. Routh, S. Voleti, S. K. Saha, M. Kumar, T. Saha-Dasgupta, and A. Paramekanti, Proximate Dirac spin liquid in the J_1-J_3 XXZ model for honeycomb cobaltates, arXiv:2212.13271.

[65] Y. Watanabe, S. Trebst, and C. Hickey, Frustrated ferromagnetism of honeycomb cobaltates: Incommensurate spirals, quantum disordered phases, and out-of-plane Ising order, arXiv:2212.14053.

[66] See Supplemental Material at http://link.aps.org/supplemental/10.1103/PhysRevB.108.L180406 for the details on the DMRG calculations, additional results, and details of the analytical MAGSWT formalism, which includes Refs. [78,79].

[67] M. Fishman, S. R. White, and E. M. Stoudenmire, The itensor software library for tensor network calculations, SciPost Phys. Codebases 4 (2022).

[68] We typically perform 16 sweeps and reach a maximum bond dimension of $m \sim 3000$ to ensure good convergence with the truncation error of $\mathcal{O}(10^{-5})$.

[69] Such symmetry breaking in DMRG mimics the 2D system, see Sec. I of the SI in Ref. [80].

[70] Z. Zhu and S. R. White, Spin liquid phase of the $S = \frac{1}{2}$ J_1–J_2 Heisenberg model on the triangular lattice, Phys. Rev. B **92**, 041105(R) (2015).

[71] Z. Zhu, P. A. Maksimov, S. R. White, and A. L. Chernyshev, Disorder-induced mimicry of a spin liquid in $YbMgGaO_4$, Phys. Rev. Lett. **119**, 157201 (2017).

[72] Z. Zhu, P. A. Maksimov, S. R. White, and A. L. Chernyshev, Topography of spin liquids on a triangular lattice, Phys. Rev. Lett. **120**, 207203 (2018).

[73] S. R. White and A. L. Chernyshev, Neél order in square and triangular lattice Heisenberg models, Phys. Rev. Lett. **99**, 127004 (2007).

[74] M. E. Zhitomirsky and A. L. Chernyshev, Colloquium: Spontaneous magnon decays, Rev. Mod. Phys. **85**, 219 (2013).

[75] S. Wenzel, T. Coletta, S. E. Korshunov, and F. Mila, Evidence for columnar order in the fully frustrated transverse field Ising model on the square lattice, Phys. Rev. Lett. **109**, 187202 (2012).

[76] T. Coletta, S. E. Korshunov, and F. Mila, Semiclassical evidence of columnar order in the fully frustrated transverse-field Ising model on the square lattice, Phys. Rev. B **90**, 205109 (2014).

[77] T. Coletta, M. E. Zhitomirsky, and F. Mila, Quantum stabilization of classically unstable plateau structures, Phys. Rev. B **87**, 060407(R) (2013).

[78] T. Holstein and H. Primakoff, Field dependence of the intrinsic domain magnetization of a ferromagnet, Phys. Rev. **58**, 1098 (1940).

[79] J. Colpa, Diagonalization of the quadratic boson Hamiltonian, Physica A **93**, 327 (1978).

[80] S. Jiang, D. J. Scalapino, and S. R. White, Ground-state phase diagram of the t-t'-J model, Proc. Natl. Acad. Sci. USA **118**, e2109978118 (2021).